PRAMANA
— journal of
physics

Vol. 66, No. 2
February 2006
pp. 455–465

Electron-confined LO-phonon scattering in GaAs-$Al_{0.45}Ga_{0.55}As$ superlattice

D ABOUELAOUALIM
L.P.S.C.M., Physics Department, Faculty of Sciences-Semlalia, BP:2390, 40000, Marrakech, Morocco
E-mail: abouelaoualim_d@hotmail.com

MS received 6 July 2004; revised 25 April 2005; accepted 20 August 2005

Abstract. We develop a theoretical model to the scattering time due to the electron-confined LO-phonon in GaAs-$Al_xGa_{1-x}As$ superlattice taking into account the sub-band parabolicity. Using the new analytic wave function of electron miniband conduction of superlattice and a reformulation slab model for the confined LO-phonon modes, an expression for the electron-confined LO-phonon scattering time is obtained. In solving numerically a partial differential equation for the phonon generation rate, our results show that for $x = 0.45$, the LO-phonon in superlattice changes from a bulk-like propagating mode to a confined mode. The dispersion of the relaxation time due to the emission of confined LO-phonons depends strongly on the total energy.

Keywords. Confined LO-phonon; scattering; superlattice; miniband; relaxation time.

PACS Nos 63.22.+m; 36.20.Kd

1. Introduction

Owing to the advances in crystal-growth techniques with dimensional control close to interatomic spacing, such as molecular-beam epitaxy and metal-organic vapour deposition, it has been possible to develop a variety of low-dimensional systems such as quantum wells, superlattices, quantum dots etc. Since the pioneering work of Esaki and Tsu [1,2], semiconductor superlattices (SLs) have received a great deal of research because of their transport properties and their technological applications in electronics devices such as novel oscillators, tunnel diodes, hot-electron transistors and electro-optical devices [3–9]. These structures involve some physics phenomena: *Bloch oscillation* [10,11] – the Bragg scattering of carriers from the Brillouin zone boundaries of crystal produces this effect; *negative differential conductivity* [12] – the Brillouin zone is too small that those met in the usual crystalline cause this effect; *modulation doping* [13–15] – a possible way to reduce scattering strength which is characterized by the form factor for interaction with phonon determined by the electron wave function along the direction perpendicular to the layer (this form factor decreases rapidly with the decrease of electron wave function, the mobility

can be enhanced); *sequential resonant tunnelling* [16] – in strong electric fields the miniband picture in a superlattice breaks down when the potential drop across the superlattice period exceeds the miniband width. When this condition is satisfied the quantum states become localized in the individual wells. The electron propagation through the entire superlattice involves sequential resonant tunnelling; *phonon resonance* [17] – at high field where a longitudinal-optical (LO) phonon mediates a transition between localized Wannier–Stark states whose energy separation equals the phonon energy, this effect is evident. This phenomenon depends in practice on a series of factors such as degree of perfection of the quantum well layers, the number distribution of impurities and the influence of electron–electron interaction.

One of the effects that has attracted the attention of a considerable number of researchers is the electron–LO-phonon interaction effect. In particular, some commonly used quantum structures, such as GaAs-$Al_xGa_{1-x}As$, are constituted by weak polar or semi-polar semiconductors such that at room temperature the polaron effects can strongly influence the optical and transport properties of these microstructures. Some results in Raman scattering, cyclotron resonance and magnetophonon resonance measurements show the dominance of electron interaction with LO phonons and reveal important information about the vibration modes in the layers forming SL [18–24]. The electron–LO-phonon interaction was found to be strongly dependent on both the geometrical shape and the parameters of the constituent materials [25,26]. The polaron effect in heterostructures of size is, however, quite different from that in bulk materials. Several theoretical studies are already reported on calculations of relaxation time due to scattering of carriers in semiconductor heterostucture by optical phonons, treating the case of single or multiple quantum wells [27–30]. In the work presented in this paper, we not only evaluate analytically an expression of the scattering time with the new analytic wave function in SL [31] treated quantum mechanically, but also study the dependence of this scattering time on the total energy.

2. Theoretical model

The electron–phonon interaction Hamiltonian in low-dimensional systems depends on the specific phonon spectra in the system and is different from the Fröhlich Hamiltonian for bulk phonon. The macroscopic dielectric continuum model [32–35] gives the functional form of the interface modes and confined half-space LO modes. The electron-confined LO-phonon interaction Hamiltonian as derived from Fröhlich interaction is given by [36,37]

$$H_{\mathrm{e-p}} = \lambda \sum_{q_\perp, n} \sum_{\alpha=\pm} \mathrm{e}^{iq_\perp \cdot r} H(z) t_{n\alpha}(q_\perp) u_{n\alpha}(z) \times [a_{n\alpha}(q_\perp) + a^+_{n\alpha}(-q_\perp)], \tag{1}$$

where $a(q)$ and $a^+(q)$ are the creation and annihilation operators for a bulk phonon in mode q, corresponding to the even $(-)$ and odd $(+)$ confined phonon modes and n is the miniband index, while the coupling

$$\lambda^2 = iC_\mu / \sqrt{V_q}, \tag{2}$$

where V is the volume. From [38], C can be written explicitly as

$$C = \left[\frac{e^2\hbar\omega_{\mathrm{LO}}}{2\varepsilon_0}\left(\frac{1}{\varepsilon(\infty)} - \frac{1}{\varepsilon(0)}\right)\right]^{1/2}, \tag{3}$$

where $\hbar\omega$ is the optic phonon of the nth miniband, $\varepsilon(\infty)$ and $\varepsilon(0)$ are the optical and static dielectric constants respectively, V is the volume and e is the electronic charge. For the slab model [32–39] $u_{n\alpha}(z)$ are defined as

$$u_{n+}(z) = \cos(n\pi z/L_{\mathrm{w}}), \quad n = 1, 3, 5, \ldots \tag{4}$$

$$u_{n-}(z) = \sin(n\pi z/L_{\mathrm{w}}), \quad n = 2, 4, 6, \ldots \tag{5}$$

$t_{n\alpha}$ is given by

$$t_{n\alpha} = \frac{1}{[q_\perp^2 + (n\pi/L_{\mathrm{w}})^2]^{1/2}}. \tag{6}$$

Finally

$$H(z) = \begin{cases} 1 \ \text{ if } \ -L_{\mathrm{w}} \le z \le L_{\mathrm{w}} \\ 0 \ \text{ otherwise} \end{cases} . \tag{7}$$

The scattering rate $W_{\mathrm{i}\to\mathrm{f}}$ appearing is obtained from the Fermi Golden Rule

$$W_{\mathrm{i}\to\mathrm{f}}(k) = \frac{2\pi}{\hbar}\sum_{\mathrm{f}} |\langle\xi_{\mathrm{f}}|H_{\mathrm{e-p}}|\xi_{\mathrm{i}}\rangle|^2. \tag{8}$$

Evaluating the matrix element in (8) with the Hamiltonian given by (1) we obtain

$$W_{\mathrm{i}\to\mathrm{f}} = \frac{\pi}{2\pi V\hbar}\left(N_{\mathrm{LO}} + \frac{1}{2} \pm \frac{1}{2}\right)\frac{e^2\hbar\omega_{\mathrm{LO}}}{q_\pm}\left(\frac{1}{\varepsilon(\infty)} - \frac{1}{\varepsilon(0)}\right) \times\delta(U^\pm)I(k_z^{\mathrm{i}}, k_z^{\mathrm{f}}, q_\perp), \tag{9}$$

where

$$I_n(k_z^{\mathrm{i}}, k_z^{\mathrm{f}}, q_\perp) = \sum_{q_\perp}\sum_{n,\alpha} |G_{n,\alpha}^{\mathrm{i}\to\mathrm{f}}(k_z^{\mathrm{i}}, k_z^{\mathrm{f}})|^2 \ |t_{n,\alpha}(q_\perp)|^2. \tag{10}$$

The δ-function represents the conservation of energy

$$\delta(U_\pm) = \delta\left(\frac{\hbar^2}{2m^*}(k_\perp^{\mathrm{i}^2} - k_\perp^{\mathrm{f}^2}) + E_{k_z^{\mathrm{f}}} - E_{k_z^{\mathrm{i}}} \pm \hbar\omega_{\mathrm{LO}}(q_\pm)\right)$$

$\mp$ denoting the absorption and emission processes. For optical phonon scattering

$$q_\pm^2 = k_\perp^{\mathrm{i}^2} \pm k_\perp^{\mathrm{f}^2} - 2k_\perp^{\mathrm{i}}k_\perp^{\mathrm{f}}\cos(\theta) + (k_z^{\mathrm{i}} - k_z^{\mathrm{f}} \mp G)^2 = cte, \tag{11}$$

where G is the reciprocal lattice vector of the SL. N_{LO} is the LO-phonon occupation number defined as

$$N_{\mathrm{LO}} = \left(\exp \frac{\hbar\omega_{\mathrm{LO}}}{k_{\mathrm{B}}T} - 1\right)^{-1}. \tag{12}$$

$G^{\mathrm{i}\to\mathrm{f}}_{n,\alpha}(k^{\mathrm{i}}_z, k^{\mathrm{f}}_z)$ is the overlap integral of the electron wave function and the z-dependent electron-confined-phonon Hamiltonian

$$G^{\mathrm{i}\to\mathrm{f}}_{n,\alpha}(k^{\mathrm{i}}_z, k^{\mathrm{f}}_z) = \int_{-L/2}^{L/2} \psi^*_{\mathrm{f}}(z) u_{n,\alpha} \psi^*_{\mathrm{i}}(z) \mathrm{d}z, \tag{13}$$

where ψ_{i}, ψ_{f} are the miniband electron envelope wave functions in the initial and final states respectively [31]. L is the period of the SL; $L = L_{\mathrm{w}} + L_{\mathrm{b}}$. At $U^{\pm} = 0$, $k^{\mathrm{f}}_{\perp}$ and $k^{\mathrm{i}}_{\perp}$ must be equal. We define a coordinate system and general lines of summation over k_{f} states that

$$\sum_{k_{\mathrm{f}}} = \frac{V}{(2\pi)^3} \int_0^{\infty} k^{\mathrm{f}}_{\perp} \mathrm{d}k^{\mathrm{f}}_{\perp} \int_0^{2\pi} \mathrm{d}\theta_{\mathrm{f}} \int_{-\pi/L}^{\pi/L} \mathrm{d}k^{\mathrm{f}}_z, \tag{14}$$

where $(k^{\mathrm{f}}_{\perp}, \theta)$ are the polar coordinates in the planes normal to k^{f}_z defined earlier with the following Jacobian

$$\frac{\partial U^{\pm}}{\partial k^{\mathrm{f}}_{\perp}} = \frac{\hbar^2}{m^*} k_{\perp}. \tag{15}$$

With the use of (9), (13) and (15) the expression for scattering time due to the electron-confined-phonon interaction τ^{-1} is calculated in first-order perturbation theory:

$$\tau^{-1}_{\mathrm{op}} = \frac{1}{\tau_0 k_{\perp}} \int_0^{2\pi} \mathrm{d}\theta \left\{ \int_{\gamma^+} \frac{I^+_{n,\alpha}(k^{\mathrm{i}}_z, k^{\mathrm{f}}_z, q_{\perp})[N_{\mathrm{LO}}(\omega) + 1]\mathrm{d}k^{\mathrm{f}}_z}{q^2_+} + \int_{\gamma^-} \frac{I^-_{n,\alpha}(k^{\mathrm{i}}_z, k^{\mathrm{f}}_z, q_{\perp})[N_{\mathrm{LO}}(\omega) + 1]\mathrm{d}k^{\mathrm{f}}_z}{q^2_-} \right\}, \tag{16}$$

where $\gamma^{\pm}$ is the integration domain over k^{f}_z and is represented in figure 1.

3. Numerical results and discussion

For numerical computation, we have chosen the GaAs-$Ga_{1-x}Al_xAs$ with $x = 0.45$ as a superlattice. The parameters pertaining to the system are: $m^*_{\mathrm{w}} = 0.067m_0, m^*_{\mathrm{b}} = 0.104m_0$, where m_0 is the free electron mass. The dielectric constant in the wells is taken equal to the one in barrier: $\varepsilon_{\mathrm{d}} = 12.8$, $\varepsilon_{\infty} = 10.9$, $l_{\mathrm{w}} = 108$ Å, $l_{\mathrm{b}} = 38$ Å, $V_{\mathrm{b}} = 495$ meV. The energy of a bulk GaAs LO phonon $\hbar\omega_{\mathrm{LO}} = 36.8$ meV, the static and high frequency dielectric constant for GaAs: $\varepsilon_{\mathrm{s}} = 12.35$ and $\varepsilon_{\infty} = 10.48$.

Figure 2 shows the plot of electron–LO-phonon coupling constant as a function of composition x. This constant increases monotonously and therefore we treat the x

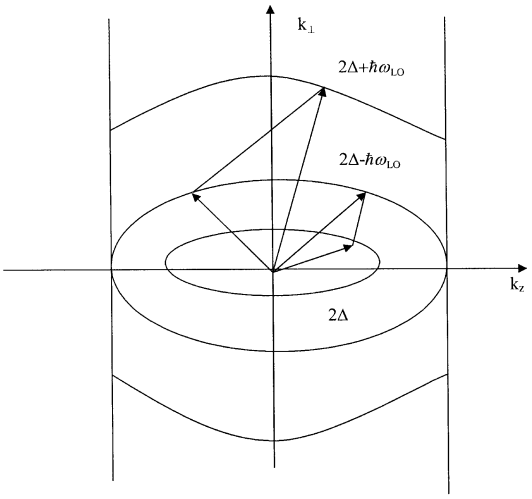

Figure 1. Representation of constant-energy lines $\varepsilon_{\xi K} = \text{const.}$ in $(k_\perp, k_z)$ plane, the difference being $\hbar\omega_{\rm LO}$. Two examples are drawn: $2\Delta + \hbar\omega_{\rm LO}$ and $2\Delta - \hbar\omega_{\rm LO}$.

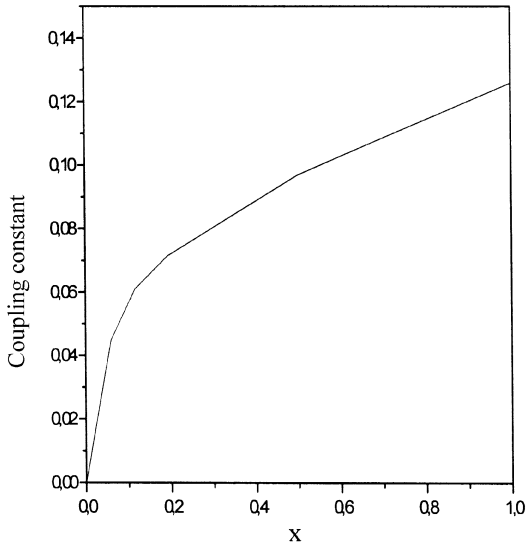

Figure 2. Variation of coupling constant as a function of composition.

fraction as the parameter for electron–LO-phonon interaction in superlattice. The variation of the optical phonon energy as a function of composition is represented in figure 3 which shows that with the increase of the concentration fraction, the optical LO-phonon energy increases. A partial differential equation is solved numerically for the phonon generation rate $(\partial N_q/\partial t)$ for $x = 0.45$.

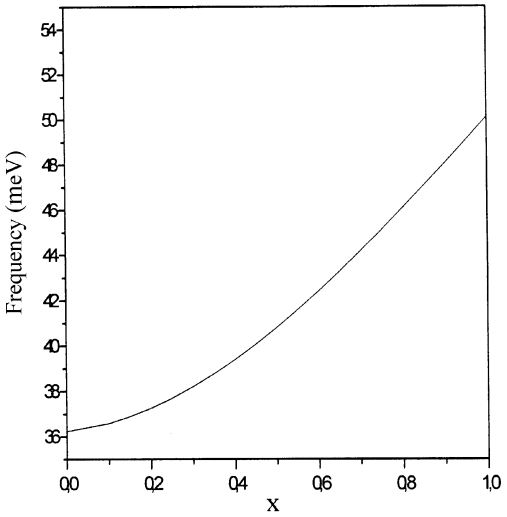

Figure 3. Optical phonon energy as a function of composition, x.

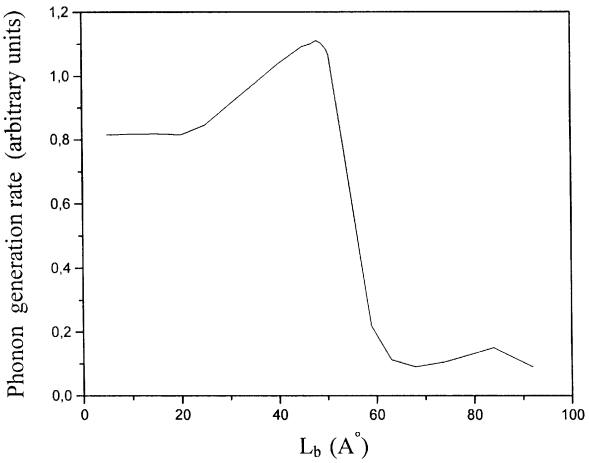

Figure 4. Representation of the phonon generation rate vs. L_{b}.

$$\frac{\partial N_q}{\partial t} = \frac{2\pi}{\hbar}(N_q+1)\sum_K |M_q|^2 f(K,t)[1-f(K-q,t)] \times\delta(\varepsilon_{\xi K-q}-\varepsilon_{\xi K}+E_{\mathrm{LO}}) - \frac{2\pi}{\hbar}N_q\sum_K |M_q|^2 f(K,t)[1-f(K+q,t)] \times\delta(\varepsilon_{\xi K-q}-\varepsilon_{\xi K}+E_{\mathrm{LO}}) - \frac{N_q}{\tau_q}. \tag{17}$$

The results are shown in figure 4. We observe a strong dependence of $(\partial N_q/\partial t)$ on the barrier width L_{b}. We deduce that the barrier width L_{b} has an effect on

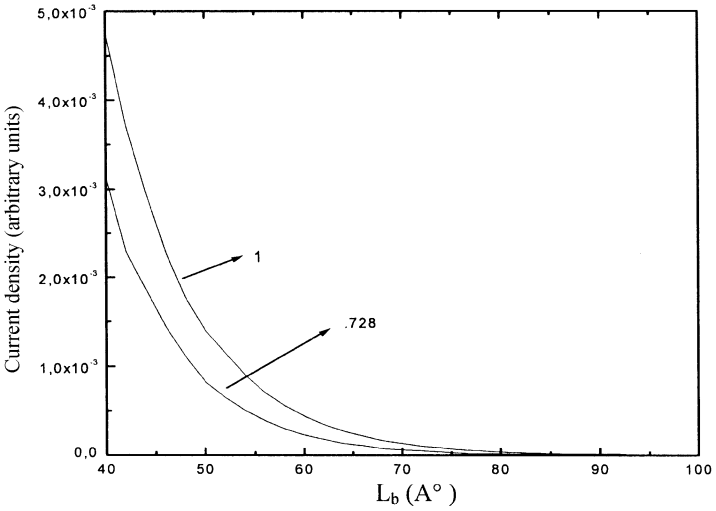

Figure 5. Current density vs. L_b for two different values of transport masses.

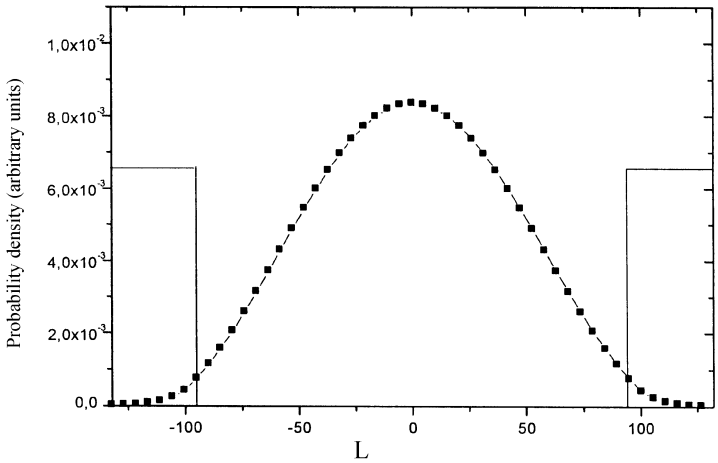

Figure 6. Probability density associated with an electron of the first miniband in the tight binding approximation. Links pace of potential is to indicate the positions of the barrier and well of superlattice.

the phonon generation rate, as well as on the confinement of the LO-phonon in the semiconductor superlattice. The variation of the current density with barrier width is plotted in figure 5 which shows that the current decreases with increasing barrier width. Accordingly, the behaviour of the tunnelling probability also decreases with increasing barrier width indicating that the electronic confinement increases. We present in figure 6 the probability density associated with an electron in the conduction miniband; which shows its maximum in the middle of the quantum wells of superlattice, where majority of electrons is found, with minimum in the barrier.

When the barrier width increases, the confinement increases. The two phenomena are competitors. The first is the contribution of interface phonon and second is the contribution of confined phonon. This competition is controlled through the factor $\Gamma = \gamma_{\mathrm{L}} L_{\mathrm{w}}$ where $\gamma_{\mathrm{L}} = (2m^*_{\mathrm{w}}\omega_{\mathrm{L}_1})^{1/2}$ is the wave vector of optical phonon parallel to the interface.

– If $\Gamma > 1$, the contribution of confined LO-phonon increases.

– If $\Gamma < 1$, the contribution of interface phonon increases resulting in the reduction of the confined contribution.

We deduce that the composition x and width of the barrier are the essential parameters in the electron–LO-phonon interaction, especially for the confinement of LO-phonon in the superlattice. It justifies our choice of parameters for numerical results. Another quantity which influences the scattering rates is the overlap integral given by eq. (13). When plotted as a function of the final wave vector for several values of initial wave vector (figure 7), for larger values of the final wave vector k_z^{f} the quantity $G_{n,\alpha}^{\mathrm{i}\to\mathrm{f}}(k_z^{\mathrm{i}}, k_z^{\mathrm{f}})$ present larger overlap integrals, resulting in increasing scattering rates. In figure 8 we present a schematic diagram of phonon wave vectors which shows that for larger energy minibands the phonon wave vectors can be larger. Since the Fröhlich interaction is roughly proportional to $1/q$, the electron couple more weakly to the phonon. Therefore, the scattering rates will be reduced. Figure 9 illustrates the scattering time due to the electron-confined LO-phonon interaction confined as a function of the total energy ε_ξ for the value of $k_z^{\mathrm{i}} = \pi/2L$.

– For $\varepsilon_1 < \varepsilon_\xi < \varepsilon_2$ the relaxation time increases with total energy of a linear way that describes the dependence of τ_{op} with energy. We can deduce that $\varepsilon_{\mathrm{i}} = |2\Delta - \hbar\omega_{\mathrm{LO}}|$ and $\varepsilon_2 = 2\Delta$.

– When $2\Delta < \varepsilon_\xi < 2\Delta + \hbar\omega_{\mathrm{LO}}$ the scattering time decreases drastically as total energy increases which is due to the confinement effect and in confirmity with a previous remark that for larger energy miniband the electron couples weakly to the phonon.

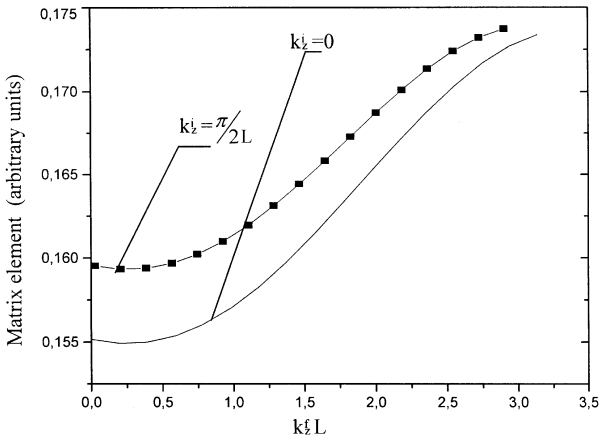

Figure 7. Plots of the matrix elements as $k_z^{\mathrm{f}}L$ for two different k_z^{i} values.

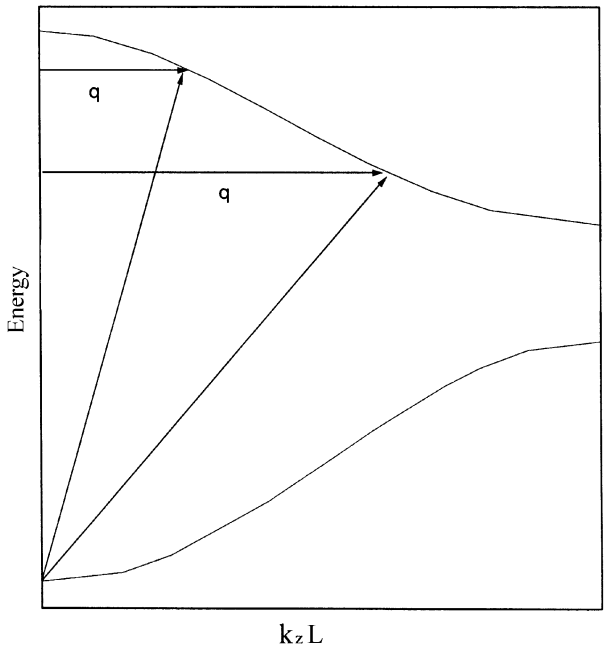

Figure 8. Schematic diagram of phonon wave vectors.

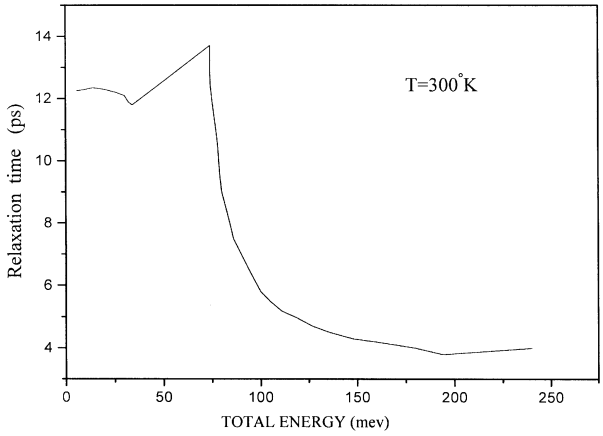

Figure 9. Relaxation time in GaAs-$Al_{0.45}Ga_{0.55}As$ superlattice as a function of the total energy for $k_z^{\mathrm{i}} = \pi/2L$.

In conclusion, we have presented a systematic study of the relaxation time due to the electron-confined LO-phonon interaction. The theory presented applied the slab model for confined LO-phonon modes, and used a new analytic wave function associated with electron in conduction minibands. We have shown that the composition x of GaAs-$Ga_{1-x}Al_xAs$ superlattice and the width at the barrier L_{b} are essential parameters and the confinement LO-phonon results are in agreement

with experimental measurements [40]. The competition between the contribution of interface phonon and the one of confined phonon is controlled through the factor Γ. We also found that the scattering time significantly depends on total energy.

References

[1] L Esaki and R Tsu, *IBM. J. Res. Dev.* **14**, 61 (1970)
[2] R Tsu and L Esaki, *Appl. Phys. Lett.* **10**, 246 (1971)
[3] L Eaves, F W Sheard and G A T Toombs, *Band structure engineering in semiconductor microstructures* edited by R A Abram and M Jaros (Plenum, New York, 1989) vol. 189, p. 149
[4] E E Mendez, *Interfaces, quantum wells, and superlattices* edited by C Leavens and R Taylor (Plenum, New York, 1988) vol. 179, p. 227
[5] P Lugli, *Band structure engineering in semiconductor microstructures* edited by R A Abram and M Jaros (Plenum, New York, 1989) vol. 189, p. 187
[6] C Y Chang, W C Liu, M S Jame, Y H Wang, S Luryi and S M Sze, *IEE Electron Device Lett.* **EDL-7(9)**, 497 (1986)
[7] R Dingle, *Semiconductors and semimetals* (Academic Press, New York, 1987) vol. 24
[8] H C Casey and M B Panich, *Heterostructure lasers* (Academic Press, New York, 1978)
[9] N Holonyak Jr., R M Kolbas and R D Dupus, *IEEE J. Quantum Electron.* **QE-16**, 170 (1980)
[10] R O Grondin, W Porod, J Ho, Ferry and G J Iafrate, *Superlattice and Microstructures* **1**, 183 (1985)
[11] E Brown, W D Goodhue, T C L G Sollner, *J. Appl. Phys.* **64**, 1519 (1988)
[12] F Capasso, K Mohamed and A Cho, *J. Appl. Phys. Lett.* **48**, 478 (1986)
[13] A C Gossard, *Molecular beam epitaxy and heterostructures* edited by L L Chang and K Ploog (Martinus Nijhoff Publishers, Dordrecht, 1985) p. 499
[14] J H English, A C Gossard, H L Störmer and K W Baldwin, *Appl. Phys. Lett.* **50**, 1826 (1987)
[15] L Pfeiffer, K W West, H L Störmer and K W Baldwin, *Appl. Phys. Lett.* **55**, 1988 (1989)
[16] M A Reed, J W Lee and H L Tsai, *Appl. Phys. Lett.* **49**, 158 (1986)
[17] D Emin and C F Hart, *Phys. Rev.* **B36**, 2530 (1987)
[18] M C Thatam, J F Ryan and C T Foxon, *Phys. Rev. Lett.* **63**, 1637 (1989)
[19] C Priester, G Allan and H Lannoo, *Phys. Rev.* **B28**, 7194 (1983)
[20] A Seilmcier, H J Hubner, G Absteiter, G Weimann and W Schlapp, *Phys. Rev. Lett.* **59**, 1345 (1987)
[21] B Jusserand and M Cardona, *Light scattering solids V* edited by Cardona
[22] G Guntherodt, *Topics Apll-Phys.* (Springer, Berlin, Heidelberg, 1989) vol. 66, p. 49
[23] M V Klein, *IEE J. Quantum Electron.* **QE-22**, 1760 (1986)
[24] B Jusserand, D Paquet and A Regreny, *Phys. Rev.* **B30**, 6245 (1984)
[25] V M Fomin and E P Pokatilov, *Phys. Stat. Sol.* **B132**, 96 (1985)
[26] E P Pokatilov, V M Fomin and N N Semenovkaya, *Phys. Rev.* **B47**, 16597 (1993)
[27] R Lassmig, *Phys. Rev.* **B30**, 7132 (1984)
[28] Xi-Xiq Liang, *J. Phys.* **C4**, 9769 (1992)
[29] Wenhui Duan, Jia-Lin Zhu and Bing-Lim Gun, *J. Phys. Condens. Matter* **5**, 2859 (1993)
[30] R Ferrira and G Bastard, *Phys. Rev.* **B40**, 1074 (1989)
[31] D Aitelhabti, P Vasilopoulos and J F Curie, *Can. J. Phys.* **68**, 286 (1990)

[32] R Fuchs and K L Klieewer, *Phys. Rev.* **A140**, 2076 (1965)
[33] A A Lucas, E Kartheuser and R G Badro, *Phys. Rev.* **B32**, 2488 (1970)
[34] E P Pokatilov and S I Beril, *Phys. Stat. Sol.* **B118**, 567 (1983)
[35] L Wendler, *Phys. Stat. Sol.* 513 (1985)
[36] J J Licari and R Evrard, *Phys. Rev.* **B15**, 2254 (1977)
[37] Khuang ad B-Fzhu, *Phys. Rev.* **B38**, 2183 (1988)
[38] M Saitoh, *J. Phys.* **C5**, 914 (1972)
[39] G Weber, *Phys. Rev.* **B46**, 16171 (1992)
[40] A Bouchalkla, Dai-Sik kim and Jin-Joo Song, *Quantum well and superlattice physics IV PIE* **1675**, 74 (1992)